FEM Application for Evaluating and Improving the Insulation System of the 33kV Wound-Core Type Distribution Transformer

Kassim R. Hameed[1] & Ibraheem J. Jabur[1]

[1] Faculty of Engineering, Al-Mustansiriah University, Baghdad, Iraq

Correspondence: Ibraheem J. Jabur, Faculty of Engineering, Al-Mustanisriah University, Baghdad, Iraq. E-mail: ibraheem.jjb@gmail.com/Kassim.r.h60@gmail.com

Abstract

This paper presents a 2-D & 3-D FE model of 250kVA, 33/0.416 kV wound core type distribution transformer, simulated using ANSYS 17.2 software in order to evaluate the insulation system via dielectric strength under power frequency and induced withstand tests and using two types of analysis, time-harmonic analysis to simulate the dielectric tests, and electro-static analysis to calculate the capacitance matrix. The assessment is based on the maximum allowable electric field intensity. the obtained results were compared with those of the real test, and the values of electric stress were less than the maximum allowable values. also, improvements to the presented model were applied following the transformer assessment. The improvement to the transformer insulation structure was done using three suggested finite element models included reduction and changing the materials type. the results were reviewed in form of contour plots, vector plots, and curves.

Keywords: electric field, FEM, Ansys, dielectric test, electric stress, CMATRIX

1. Introduction

1.1 General Introduction

The insulation system is one of the important parts of a transformer, since its malfunctioning leads to transformer failure. The good insulation structure of a distribution transformer determines that a transformer normally operating during transformers lifetime (Mladen M., et al, 2013). In spite of the improvements done on the insulation materials used in transformer had enabled higher withstand voltages, engineers try to find new design rules to catch up with ever demanding task for increasing the profit and reduce the cost. With the use of modern computers, numerical calculations have become one of the prime tools for solving complicated engineering problems with the goal for improvement in component design and better quality of the final product (Mladen M., et al, 2013). The critical parameter in the breakdown of an insulator is the electric stress, because the minimum thickness required between conductors, and the conductors and the ground, the insulation level is depending on the value of the maximum electric stress (Aydemir A., Özcan K., 2005). Continues efforts has been made to improve and as a result reduce the insulation content in the transformers to satisfy the increasing competition in the global market, but care must be taken when the insulation content is reduced to avoid potential risks or else, transformers will fail to continue operation (Kosjenka C., et al., 2013).

In this research, the insulation structure classified into three categories, the H-L insulation (insulation between high voltage windings and the low voltage windings), the H-C insulation (between the high voltage windings and the iron core), and the H-H insulation (between the high voltage windings and the high voltage windings of the adjacent phase). Also two types of FEM models were suggested as an improvement to the insulation structure of the transformer under study, in the first model, the insulation distances were reduced and maintaining the maximum value of electric field intensity located on the FEM model is less than the breakdown values. The second suggested model was done by creating oil gaps within the press-board layers in the H-H insulation and the H-C insulation but the insulation thickness was kept unchanged, this has reduced the maximum values of electric field intensity at both the H-H and H-C insulation.

1.2 Literature Survey

(Alireza K., & Mehdi V., 2008), investigated insulation design improvements by representing 230 kV transformer windings with lumped parameter equivalent model using FEM. Their design criteria were also based on maximum

electric field. This paper shows how insulation distances can be decreased using oil breakdown criteria, through FEM and BEM. (Youhua G., et al, 2011; Youhua G., Shaobo W,2012), studied the effect of changing the insulation distances of 110kV power transformer by determining the maximum allowed electric stress. (Linsuo Zeng et. al, 2009), in this research, 2-D and 3-D finite element model is implemented in order to analyze the HV lead of 400kV power transformer using ANSYS software. from the results obtained, the maximum value and position of electric field is located on the finite element model, and the distribution of electric field in all the parts of the finite element model is visually illustrated.

1.3 Dielectric Tests

A distribution transformer needs to withstand specific standard of overvoltages to be reliable during its lifetime. This can be established through dielectric tests. According to International Electrotechnical Commission (IEC) standard 60076-3, there are two/ types of dielectric tests: separate source (AC, 50 Hz), induced withstand voltage tests. For each type of test, amount of voltage and time of test are regulated by the standard. For instance, separate source AC duration is one minute, and induced tests may last from twenty minutes to one hour (Mladen M., et al, 2013).

2. Finite Element Transformer Model

The 250kVA/33kV wound-core type distribution transformer was simulated using ANSYS multi-physics which is a programs uses finite element method for the analysis and obtaining the results. Finite element method is considered as one of the numerical analysis that used to solve differential equations that approximately describe or to describe a wide number of physical problems such as electric-magnetic fields, fluid, solid and soil mechanics (Sivaji Chakravorti, 2015).

The transformer model was simulated in ANSYS software, and figures 1& 2 show the 2-D transformer model and the mesh pattern respectively. All the dimensions of the 250kVA/33kV wound-core type distribution transformer is taken from the documentaries of Dyala company for electrical industries (Dyala Company for Electrical Industries, 1983).
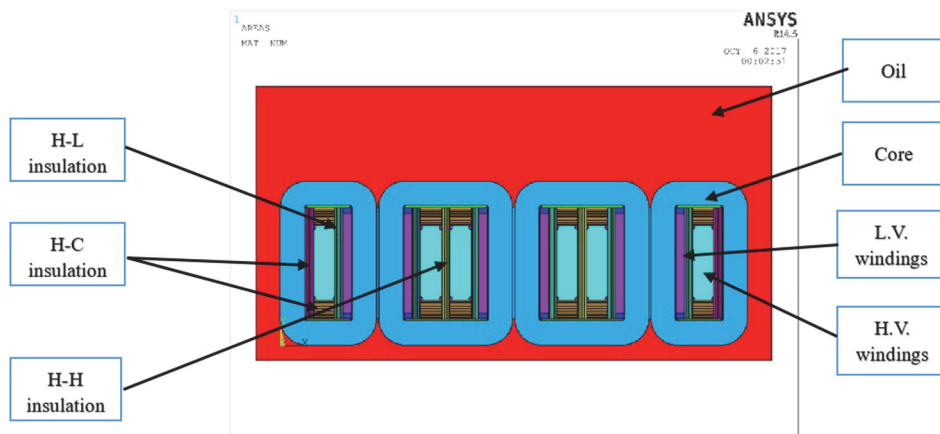

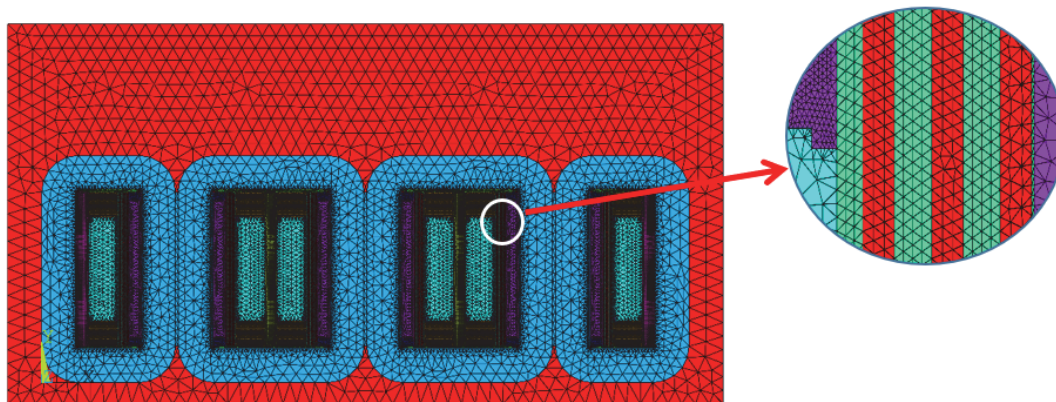Figure 1. Transformer active part with insulation system

Figure 2. Mesh pattern of the transformer active part with insulation system

The thickness between the high-voltage windings and the low-voltage windings of each phase is 20mm, the thickness between the high-voltage windings and the transformer core from the sides is 23.5mm while from the top and the bottom is 51mm, the gap distance between the high-voltage windings of different phases is 22mm (Dyala Company for Electrical Industries, 1983).

2.1 Boundary Treatment

In order to analyze the electric field and obtain accurate results, the need to give the appropriate material properties and the appropriate boundary conditions arises. If the dimensions of the FE model accurate this will lead to more accurate obtained results (Youhua G., et al, 2011). For the dielectric withstand test (power frequency test), the applied boundary conditions are represented by grounding both of the low-voltage windings and the iron core, in another word the nodal potential of both the low-voltage windings and the iron core is set to zero, while the high-voltage windings were fed by 70kV (r.m.s) for 1 minute (International Electrotechnical Commission Standard 60076-3, 2013).

For the dielectric induced withstand test the applied boundary conditions represented by grounding the iron core, the low-voltage windings fed by 480V (r.m.s) which is two times the phase value since the low-voltage windings are star connected, the induced voltage on the high-voltage windings would be 66kV (r.m.s).

2.2 Governing Equations for Electric Field Analysis

The calculation of electric field for both tests satisfies Laplace equation:

$$\nabla^2 V = 0 \tag{1}$$

the relation between the electric field and the potential is as follows:

$$E = -\nabla V \tag{2}$$

And the relations between the electric field and the current density, and the electric field and the electric flux density are:

$$J = \sigma E \tag{3}$$

$$D = \varepsilon E \tag{4}$$

And by taking the divergence to both sides of the continuity equation the result is (ANSYS 17.2, 2016):

$$\nabla . (\{J\} + \{\frac{\partial D}{\partial t}\}) = 0 \tag{5}$$

By substituting equations (3) & (4) into (5), the result is:

$$-\nabla . ([\sigma]\nabla V) - \nabla . \left([\varepsilon]\nabla \frac{\partial V}{\partial t}\right) = 0 \tag{6}$$

For observing power frequency test in ANSYS, a time harmonic electric field analysis is selected and, thus equation (6) becomes:

$$-\nabla . ([\varepsilon].V) + \frac{j}{\omega}\nabla . ([\sigma]\nabla . V) = 0 \tag{7}$$

Where:

$$\omega = 2\pi f \ (rad)$$

2.3 CMATRIX Macro for Capacitance Calculation

Capacitance is defined as a configuration of conductors separated by a dielectric material, and used to store energy in form of electric field. In ANSYS software, the calculation of the capacitance value is done through the use of the CMATRIX macro, which is a command provided by the software to determine the capacitances values in form of lumped capacitance matrix, and the basis in calculating the capacitances is the energy principle.

The electro-static energy for a linear three electrodes (where the third electrode is considered to be the grounded conductor) is as follows:

$$W = \frac{1}{2}C_{11}^g V_1^2 + \frac{1}{2}C_{22}^g V_2^2 + C_{12}^g V_1 V_2 \qquad (8)$$

Where:

W: represents the stored energy.

V_1: potential of the first electrode

V_2: potential of the second electrode

C_{11}^g: self-ground capacitance of the first electrode

C_{22}^g: self-ground capacitance of the second electrode

C_{12}^g: mutual-ground capacitance between the two electrodes

After applying the appropriate voltage on the electrodes, the values of the capacitances can be obtained from the stored static energy. The next figure illustrates the lumped parameter circuit.
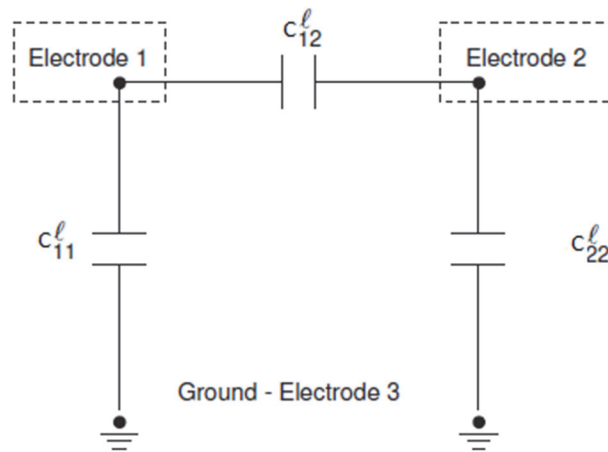
Figure 3. Lumped parameter circuit diagram

3. Results and Analysis

To evaluate an insulator and decide that the insulator works as required, the electric stress for that insulator must not exceed the allowable maximum value of electric stress at which the insulator will fail. The H-L insulation consists of varnish paper layers; the H-C insulation consists of press-board layers. The electric properties that were given for each material is illustrated in the following table. The electric properties for both insulating paper and press-board paper were oil-immersed measures (Naoki H., et al., 2006).

Table 1. Electrical properties of insulating materials

	Relative Permittivity	Resistivity	Loss Tangent
insulating paper	3.5	2.4×10^{15}	39×10^{-4}
Press-board	4.4	10^6	50×10^{-4}
Transformer oil	2.2	7.6×10^{15}	10^{-4}

In order to study the dielectric response of the insulation system, two cases were considered, the first case is that the insulator between any two conductors model consists a single dielectric material, the other case is that, the insulator consists from multi dielectric materials or layers, which is the actual case.

3.1 Results of Dielectric Withstand Tests

The dielectric withstand test (power frequency test) was carried on in the ANSYS program and the results shows that the electric stress obtained from the FE solution of the insulating paper is 2.73kV/mm while the maximum value of electric stress located in the FE model is 6.81kV/mm, while the electric stress at which the breakdown occur is 8kV/mm which is practically obtained and also determined practically by (Youhua G., et al, 2011). Figures 4 & 5 show the potential and electric field distribution respectively in insulation structure of the transformer under study.
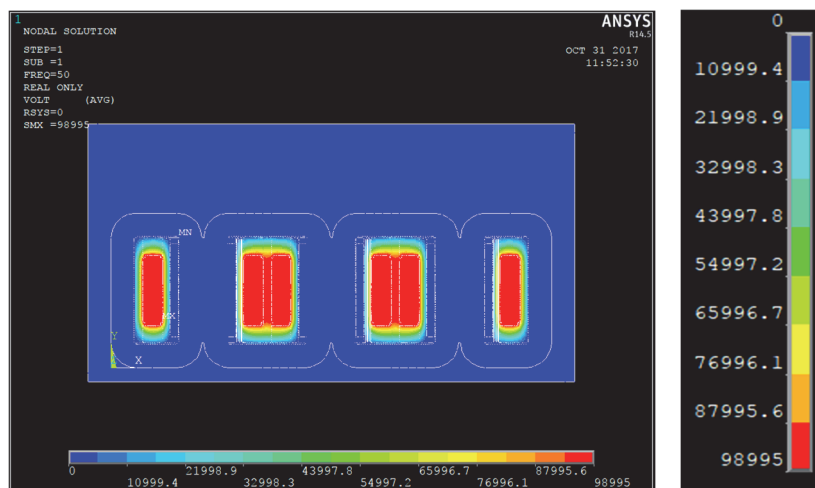
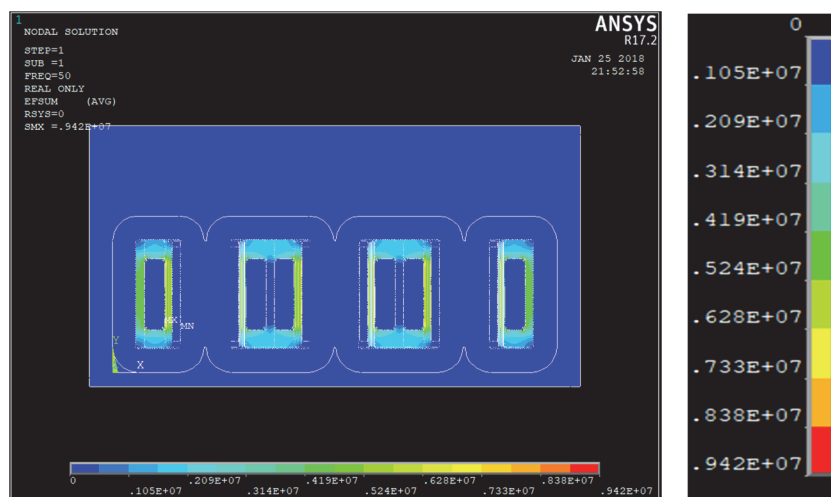Figure 4. Potential distribution in transformer insulation

Figure 5. Electric field distribution in transformer insulation

In order to determine the potential distribution and the electric field distribution between the high voltage and the low voltage windings, three different paths were considered, as shown in figure 6.
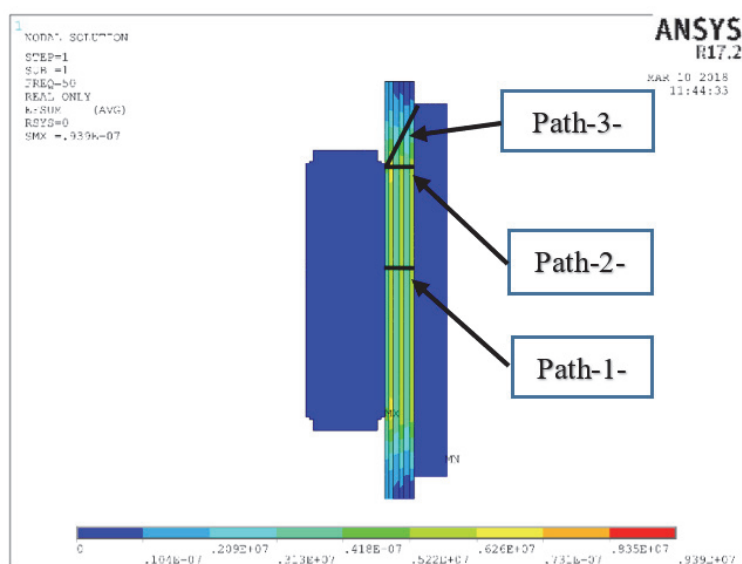
Figure 6. Electric field distribution in H-L insulation with the selected paths

the first path is located at the middle region of insulation between the high-voltage windings and the low voltage-windings. Figure 7, shows the H-L insulation at path -1- of H-L insulation, the potential distribution, and the electric field distribution for the given path.

(a)   (b)   (c)
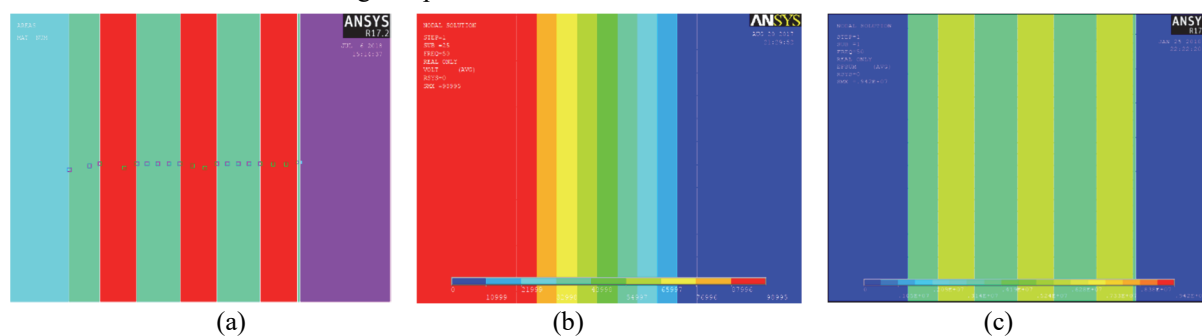
Figure 7. (a) H-L insulation at path -1- of H-L insulation. (b) contour plot of potential distribution along path -1- of H-L insulation. (c) contour plot of electric field distribution

Figures 8, show the voltage gradient and the electric field distribution of the middle region of the H-L insulation.

(a)   (b)
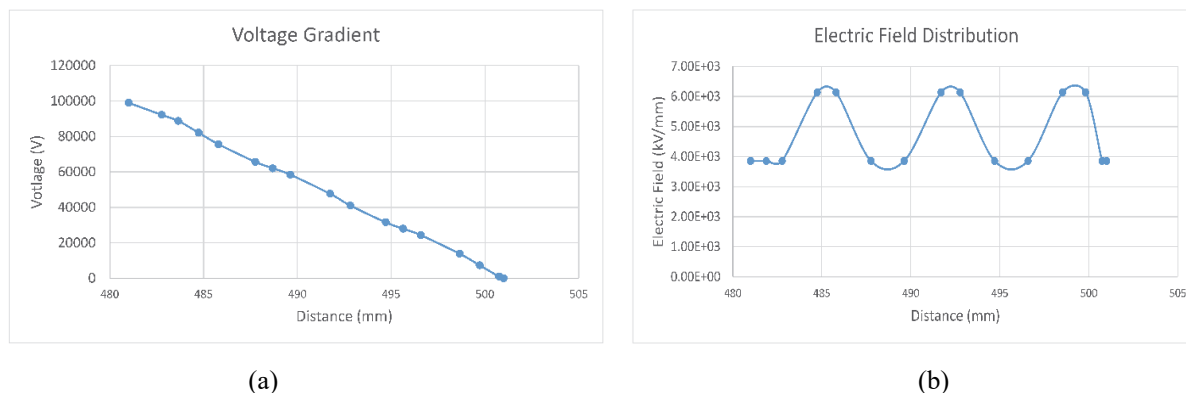
Figure 8. (a) voltage gradient along path -1- of H-L insulation. (b) electric field distribution along path -1- of H-L insulation

In figure 8-a, the presence of the gaps filled by oil makes the voltage gradient across each materials differs from the other due to their different relative permittivities, thus, the electric stress along path -1- will the fluctuate in its value due to the presence of the gaps filled by the transformer oil in the H-L insulation as shown in figure 8-b. From these curves it can be noticed that, the electric field distribution is regular due to the regular distance between the equipotential lines as shown in figure 7.

The second path chosen for studying the dielectric response of the H-L insulation is the end region of the high-voltage windings as shown in figure 9.

(a)   (b)   (c)
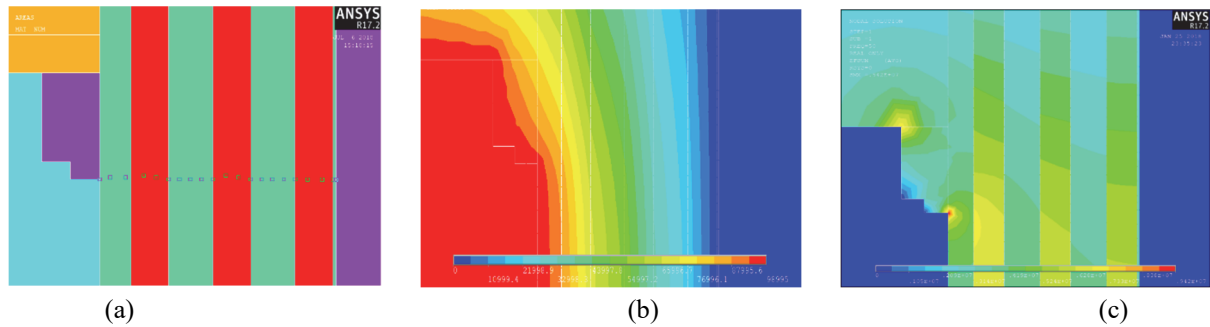
Figure 9. (a) H-L insulation at path -2- of H-L insulation. (b) electric potential along path -2- of H-L insulation. (c) contour plot of electric field distribution

The maximum value of the electric stress approximately 6.66kV/mm as illustrated in figure 8. it can be seen that the potential distribution is non-linear at the region of path -2- of H-L insulation shown in figures 10-a & 12-a. This non-linearity is because the distances between the equipotential lines is not equal, this makes the distribution of the electric field non-uniform.

The curves below show the voltage gradient and the electric field distribution respectively for the selected path.

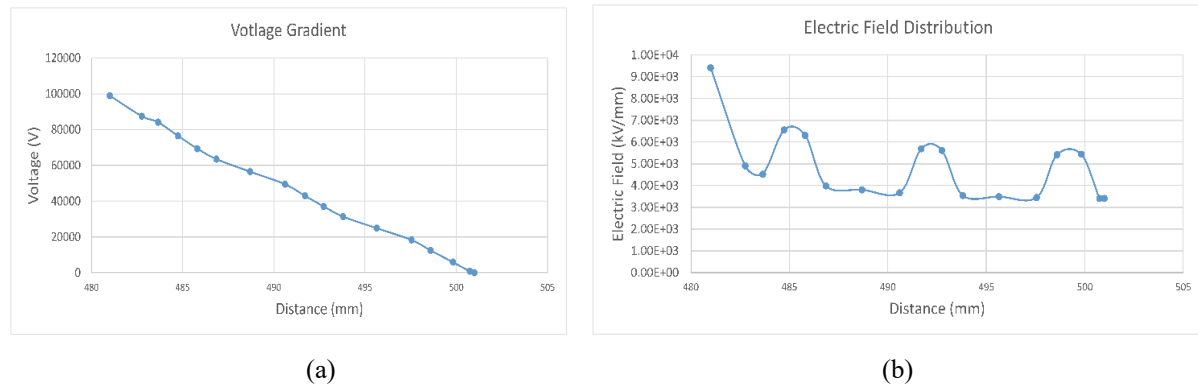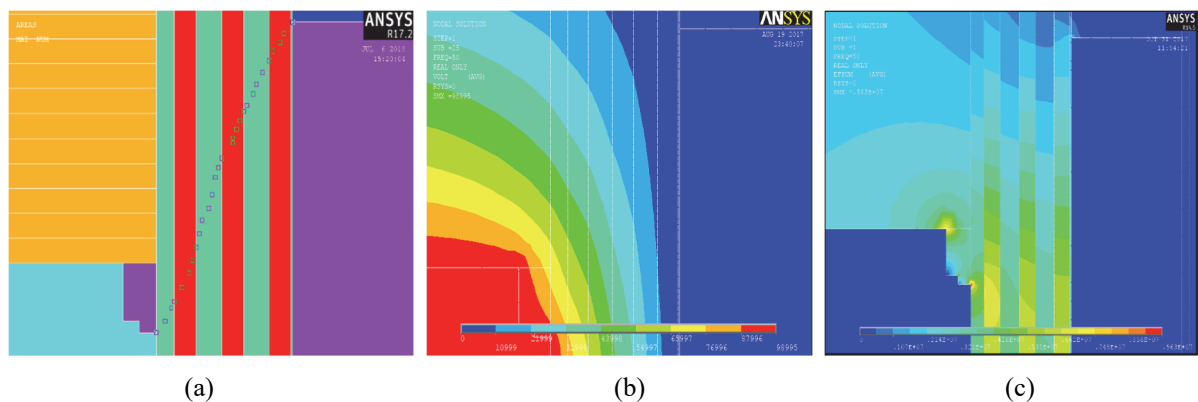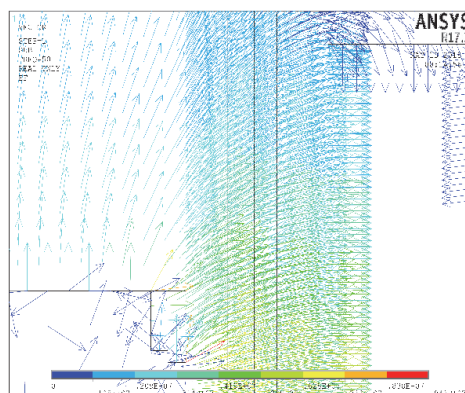(a)   (b)

Figure 10. (a) Voltage gradient at path -2- of H-L insulation. (b) electric field distribution at path -2- of H-L insulation

(a)   (b)   (c)

(d)

Figure 11. (a) 2-D model of transformer at path -2- of H-L insulation. (b) contour plot of potential distribution at path -2- of H-L insulation. (c) contour plot of electric field distribution path -3-. (d) electric field vector representation

The third path chosen to study the dielectric response was between the end regions of both high-voltage windings and the low-voltage windings. Figure 11 shows the 2-D model of the selected path from the FE model, potential distribution and the electric field distribution.

From figure 11, it can be seen that the electric stress fluctuates along the insulation thickness and this fluctuation is also due to the presence of the gaps that filled by the transformer oil, also the distribution of the electric field at the end sides of the both high-voltage windings and the low-voltage windings is irregular for the same reason discussed for path -2-, because the distances between the equipotential lines is not equal, and there for, the stress on the end sides of the high-voltage windings is greater than the stress determined in path -2- and start to decrease when approaching to the low-voltage windings. the following curves show the potential distribution and the electric field distribution respectively along the selected path.
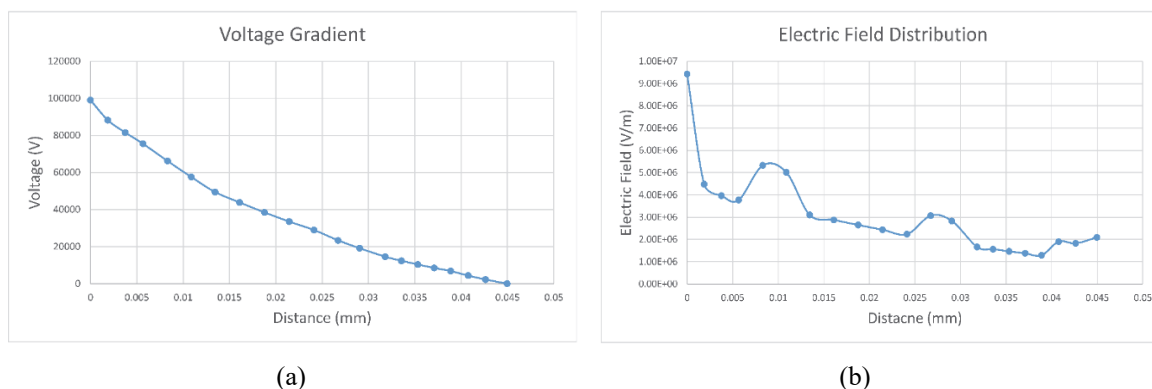
(a)

(b)

Figure 12. (a) Voltage gradient of H-L insulation at path -3-. (b) electric field distribution at path -3- of H-L insulation

For the H-C insulation, three paths were chosen to study the dielectric response of the H-C insulation as shown in figure 13.
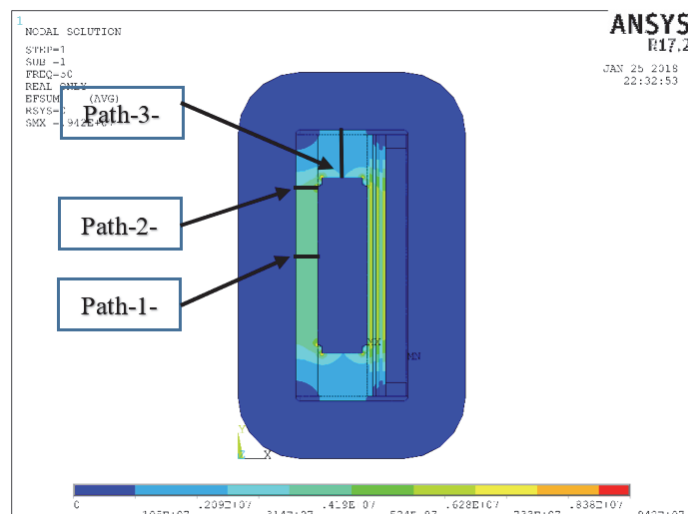
Figure 13. H-C insulation illustrating the selected paths for studying the dielectric response

It was noted that when the thickness of the H-L insulation is 20mm the electric stress within each millimeter is 2.73kV/mm, thus for the H-C insulation from the top and the bottom of the high-voltage windings, which is 51mm, the insulation works properly for this test. From figure 13, path -1- is located at the middle region between the high voltage windings, and the iron core. The thickness of this insulation at this region is 23.5mm, figure 14 shows the 2-D model of transformer at path -1- of H-C insulation, the contour plot of the potential distribution, and the electric field distribution of the given path.
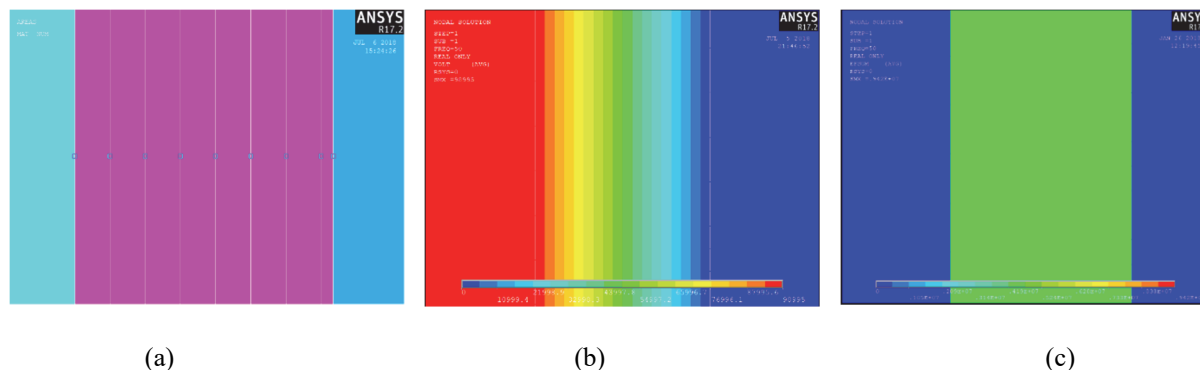

(a)　　　　　　　　　　　　(b)　　　　　　　　　　　　(c)

Figure 13. (a) H-C at path -1-. (b) contour plot of potential distribution at path -1- of H-C insulation. (c) contour plot of electric field distribution
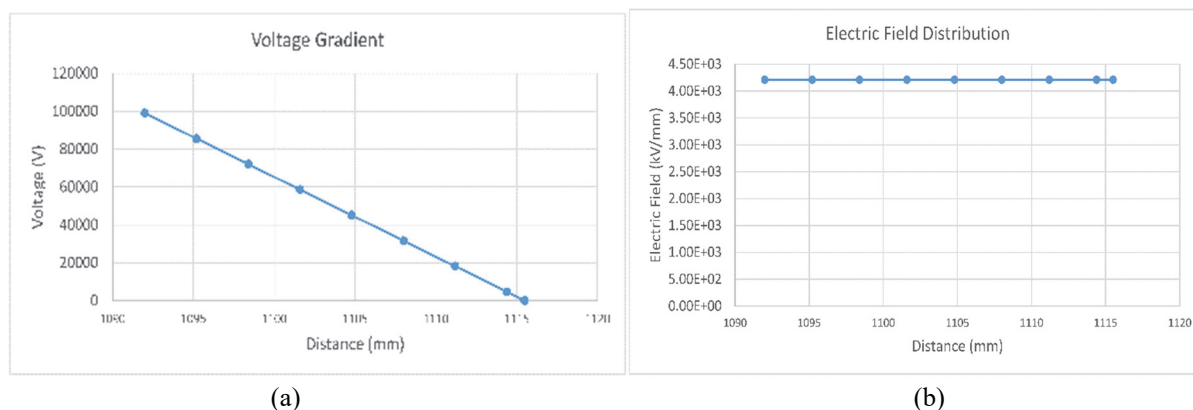

(a)　　　　　　　　　　　　　　　　　　(b)

Figure 15. (a) Voltage gradient at path -1- of H-C insulation. (b) electric field distribution along path -1-

In figure 15-a below, the gradient in voltage at path -1- of H-C insulation is the same for each millimeter along the insulation distance, because of the fact that H-C insulation is consisted of only press-board layers, and as a result the electric stress across the insulation thickness is approximately the same and there for distribution of electric field has regular distribution as shown in figure 15-b.

path -2- is located at the side region of the high voltage windings, the maximum value of electric stress in the H-C insulation is located at this path and it is equal to 5.617 kV/mm, while the breakdown value measured for the press-board paper is 9.5kV/mm. figure 16-a shows that the gradient in voltage is non-linear, this non-linearity is because the distances between the equipotential lines is not equal, and there for, the stress on the end sides of the high-voltage windings and that make the voltage within each millimeter is approximately not equal, thus the electric stress within each millimeter has different values start at its maximum values at the high voltage corners of the high voltage windings and decreases when approaching the iron core, as shown in figure 16-b.
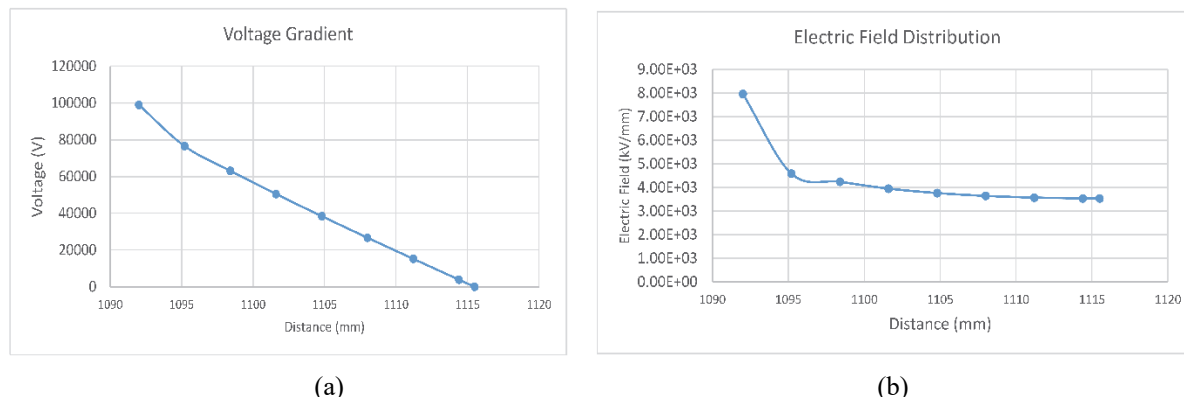

(a)   (b)

Figure 16. (a) voltage gradient at path -2- of H-C insulation. (b) electric field distribution at path -2- of H-L insulation

The next figure shows the practical transformer test that was done in the factory of distribution transformers of Dyala company. Also the value of the displacement current measured throughout the test should be within the range (0-50mA) and the value of the displacement current determined from the finite element solution was 32.5mA.

Figure 17 practical withstand test for the distribution transformer under study

3.2 Results of Dielectric Withstand Induced Test

This test was carried on in ANSYS program, and with this test the H-H insulation and the insulation between every two conducting layers of high voltage windings can be studied. Figures 18 & 19 show the potential distribution and the electric field distribution in the insulation system, when the transformer is subjected to the dielectric induced withstand test.
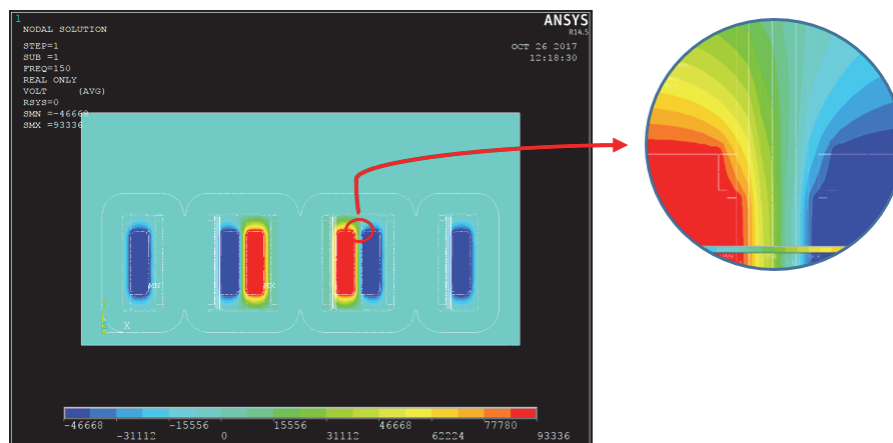
Figure 18. potential distribution in transformer insulation system under dielectric induced voltage test
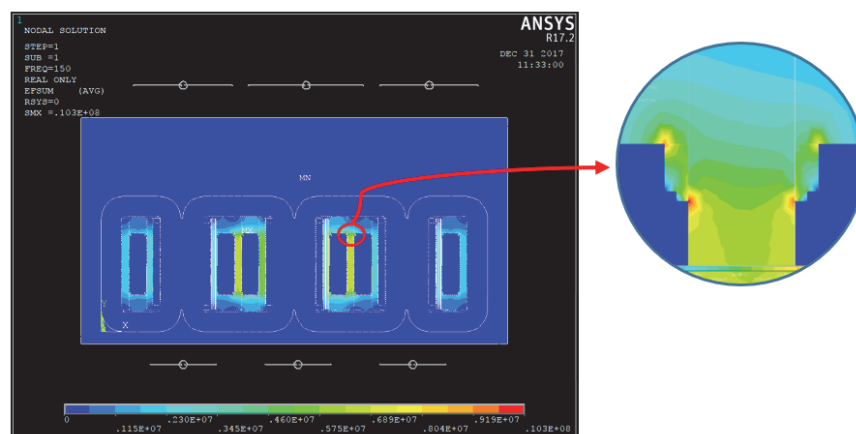

Figure 19. Electric field distribution of transformer insulation system under dielectric induced voltage test

For evaluating the performance of the H-H insulation, two paths were selected for this purpose. The first path was the middle distance between the high-voltage windings and the high voltage windings of the adjacent phase, figure 20 shows the selected paths and the distribution of the electric field.
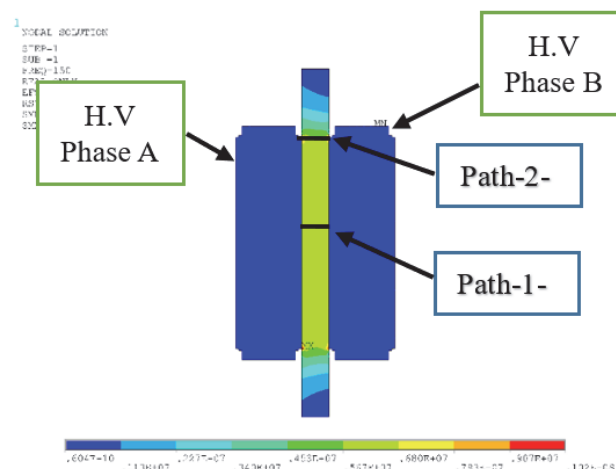

Figure 20. Electric field distribution in H-H insulation with the selected paths

In figure 21, the electric field at the path -1- of H-H insulation has a regular distribution and the stress at each point through the insulation thickness equals to 4.5kV/mm because it consists of only press-board layers, this also can

be seen from figure 22 which illustrate the voltage gradient and the electric field distribution respectively through the insulation thickness.
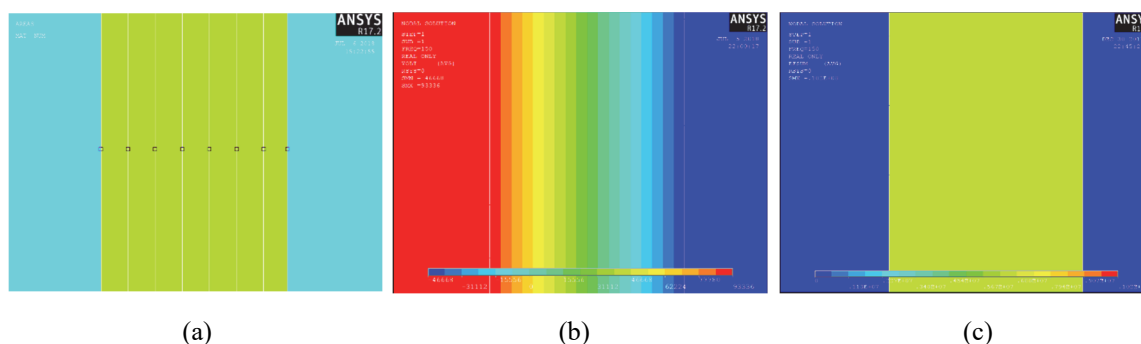

(a)   (b)   (c)

Figure 21. (a) 2-D model of transformer at path -1- of H-H insulation. (b) electric field distribution at path -1- of H-H insulation. (c) contour plot of electric field distribution
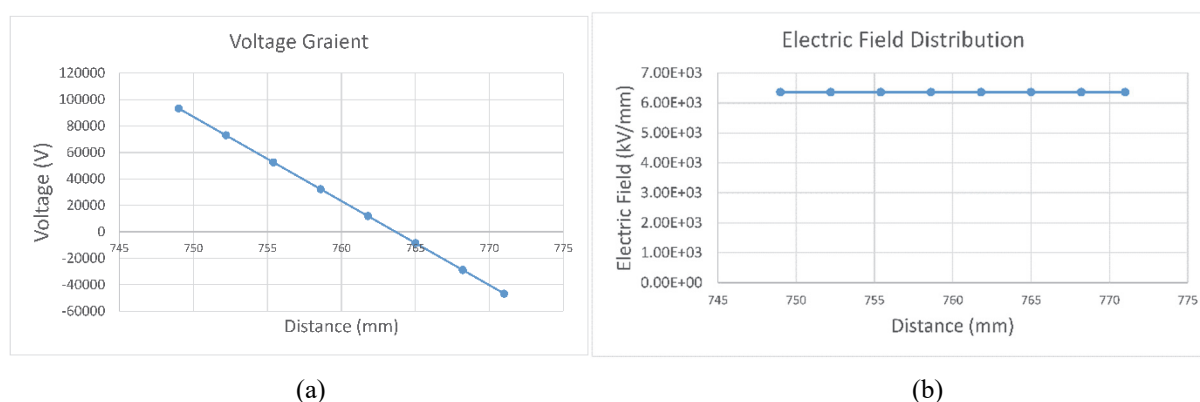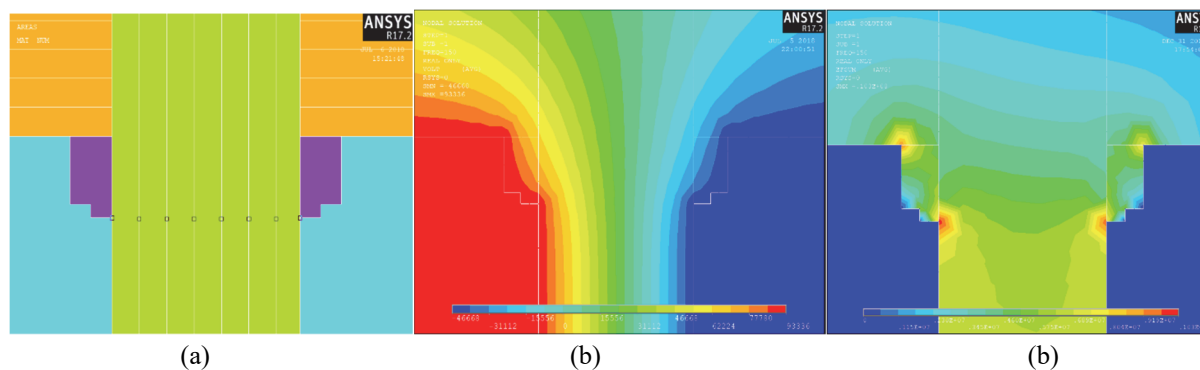

(a)   (b)

Figure 22. (a) Voltage gradient at path -1- of H-H insulation. (b) electric field distribution at path -1- of H-H insulation

The second path that is selected at the corner end of the region high-voltage windings of adjacent phases, as shown in figure 23.

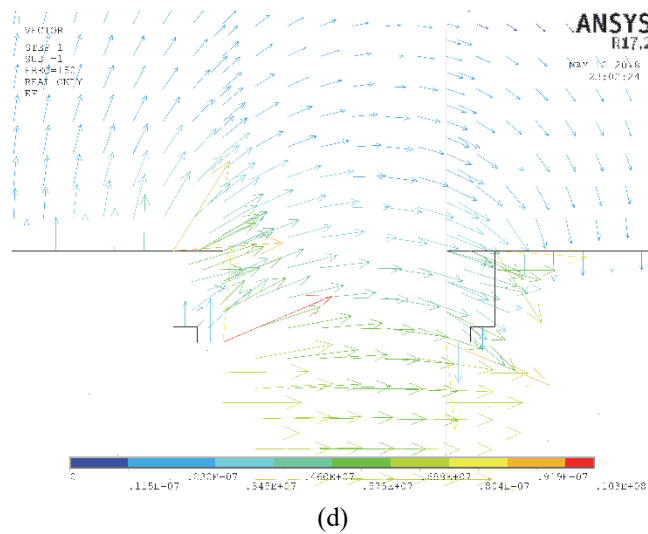

(a)   (b)   (b)

(d)

Figure 23. (a) path -2- of H-H insulation. (b) contour plot of potential distribution at path -2- of H-H insulation. (c) contour plot of electric field distribution. (d) electric field vector representation

From the figure 23 above it can be noticed that the distribution of the electric field is not regular, , this is because the side region of the H-H insulation the distances between the equipotential lines at the windings edges is smaller as compared with those at path -1- pf H-H insulation there for, the electric stress along path -2- has the minimum value at the middle distance and start arising when approaching to the edges adjacent phase whether it is A or C phase, also in this region, the maximum value of electric field is noticed at exactly the end sides of the high voltage windings of phase A and it is equal to 7.2kV/mm while the breakdown electric stress measured practically equals 9.6kV/mm. figure 24 shows the voltage gradient and the electric field distribution along path -2-.

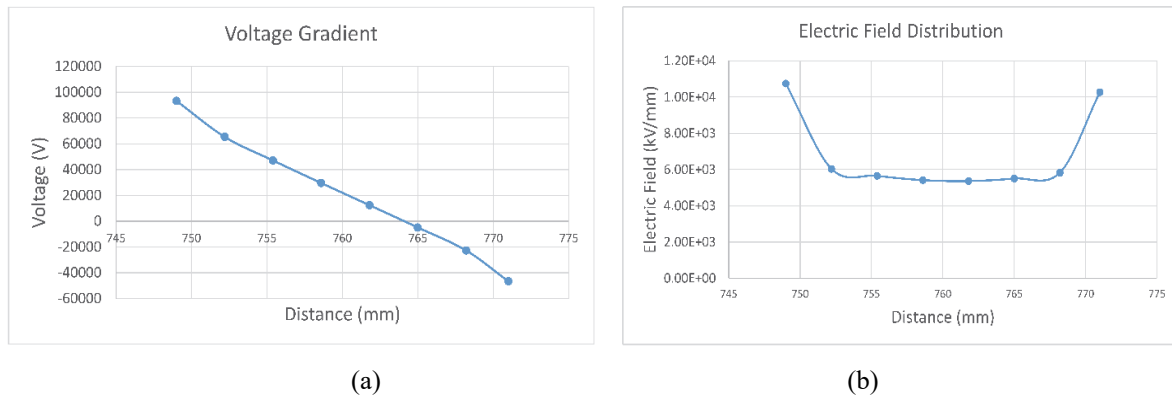

(a)   (b)

Figure 24. (a) Voltage gradient at path -2- of H-H insulation. (b) electric field distribution at path -2- of H-H insulation

As for the H-L insulation, the dielectric response as also determined due to dielectric induced withstand test, and the results show that the electric stress values are less as compared with those obtained in the separate source AC dielectric withstand test. For path -1- of H-L insulation the electric stress at the insulating paper equal to 2.55kV/mm which is less as compared with the value obtained from the dielectric AC withstand test that equals to 2.7kV/mm and the distribution of electric stress across the insulation thickness is the same behavior shown in figure 8.

For path -2- of H-L insulation, the maximum value of electric stress is appeared at this path and it equals to 6.1666kV/mm and it is less than the values obtained from dielectric AC withstand test which is 6.56kV/mm, and the distribution of electric stress along the given path has the same behavior of that shown in figure 12.

The dielectric response of the layer insulation of the high voltage windings has been determined after solving the 2-D quarter model that represents the layers of the high voltage windings. The results show that the maximum

values of electric stress located on the FE model is at PVC insulating material of the turn that has the maximum nodal voltage, and it is equal to 9.63kV/mm, while the breakdown value equals to 10.8kV/mm which was obtained by (Pugazhendhi S., 2013). Also the stress at the insulation between layers at the terminals equal to 2.8kV/mm while the electric stress at the insulation between layers of the inner windings equal to 2.7kV/mm and these values are less than the breakdown stress value of the insulating paper which equals 8kV/mm. figure 25 below shows the contour plot and vector plot for the electric field distribution of the layer insulation of the high voltage windings.
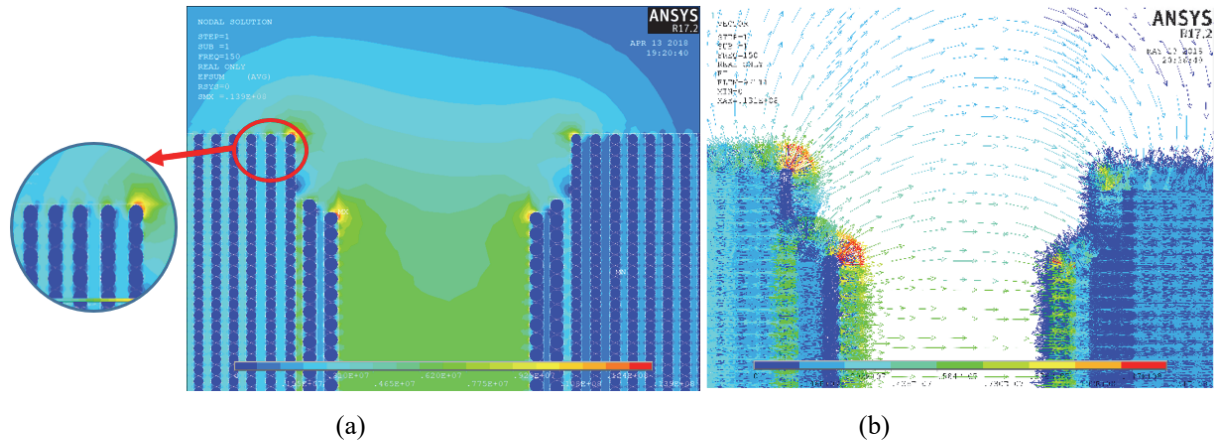

(a)   (b)

Figure 25. (a) contour plot of electric field. (b) vector representation of the electric field

3.3 Results of Capacitances Calculation

In order to determine the capacitances values, the capacitances among transformer windings and among the transformer windings and the ground are calculated as follows:

1. equivalent capacitance between the high voltage windings and the ground (iron core + oil tank) and denoted by C_{HG}.

2. equivalent capacitance between the high voltage windings and the low voltage windings and denoted by C_{HL}.

3. equivalent capacitance between the low voltage windings and the ground and denoted by C_{LG}.

The capacitances were calculated using the 3-D quarter model of the transformer shown in figure 27, and the obtained results were compared with those of the real test as shown in figure 26. Table 2 shows the values of the equivalent capacitances as compared with the actual test.
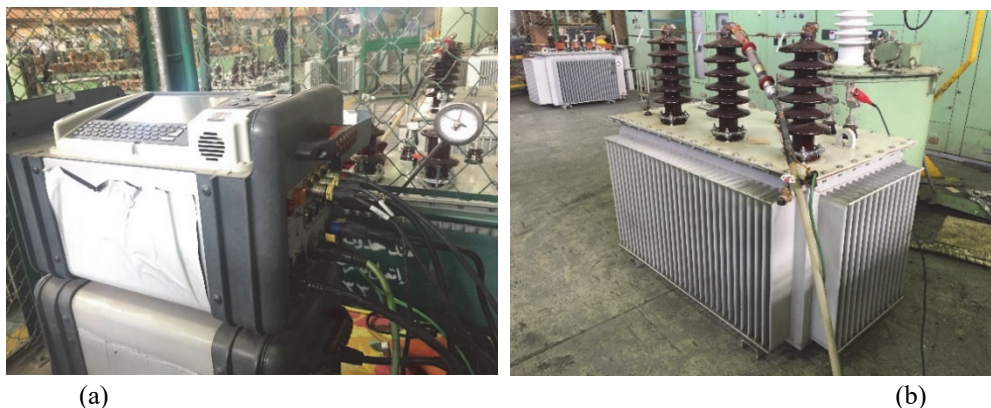

(a)   (b)

Figure 26. (a) Megger Delta4000 capacitance/tan(δ) test system. (b) distribution transformer under capacitance test

Table 2. equivalent capacitance of the distribution transformer compared with FEM results

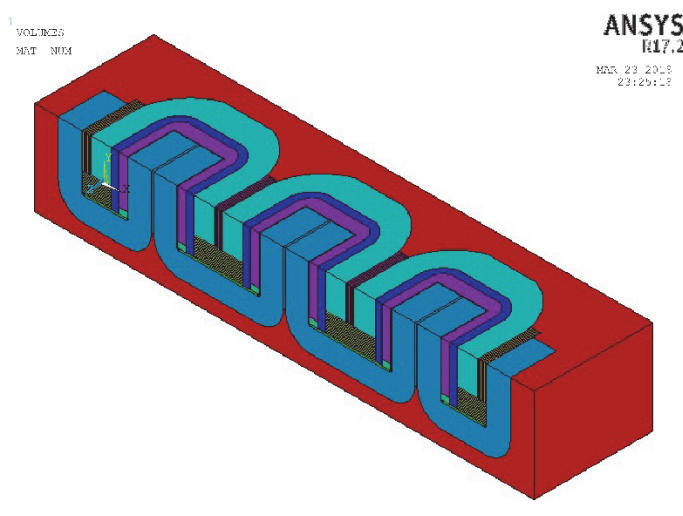|	Practical test (pF)	FEM (pF)
C_{HG}	893	630
C_{HL}	934	924
C_{LG}	4654.13	4850.5

Figure 27. 3-D quarter model of the transformer under study

The difference in the value of C_{HG} is due to the complex geometry of insulation between the high voltage windings and the ground, because in real case, transformer windings may deviate a little from their position, or another possibility that could be the cause, is the transformer oil may contain a copper-sulfur particle that can reduce the transformer oil insulation to withstand the high electric stresses and as a result, the capacitance value get changed.

3.4 Insulation System Improvement

The results obtained from simulating the separate source dielectric AC withstand test and the dielectric induced withstand test in ANSYS, show that the insulation system withstands properly and the maximum values of the electric stress in each test is less than the breakdown values. Thus, an improvement to the insulation structure can be applied.
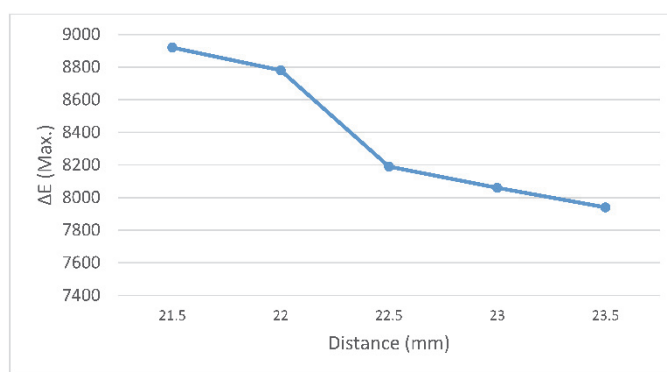

Figure 28. variation of maximum electric stress along with changing the H-C thickness

The improvement involves three FE models. In the first model the insulation thickness of the H-C insulation and the H-H insulation have been reduced 2mm in steps of 0.5mm, then the dielectric response of the H-C insulation was determined through the dielectric AC withstand test, and the dielectric response of the H-H insulation was determined through the dielectric induced withstand test. Because the electric stress and insulation thickness are inversely proportional, the electric stress values were increased when the insulation distances reduced, but values of electric stress in all regions were maintained below the breakdown limits. Figures 28 & 29 show the variation

of maximum values of H-C insulation and the H-H insulation along the insulation distances. figure 30 shows the contour plot of the entire model corresponding to the separate source AC withstand test.
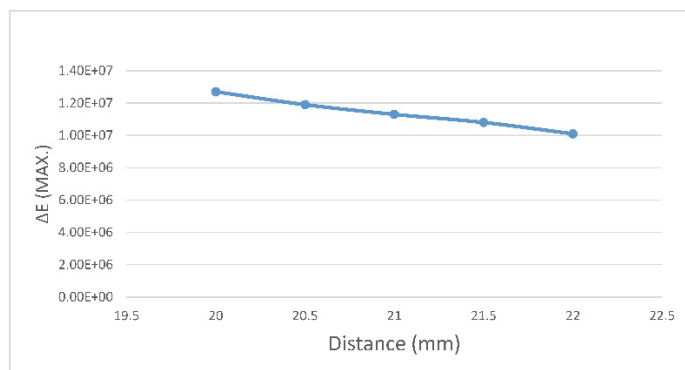

Figure 29. variation of maximum electric stress along with changing the H-H thickness
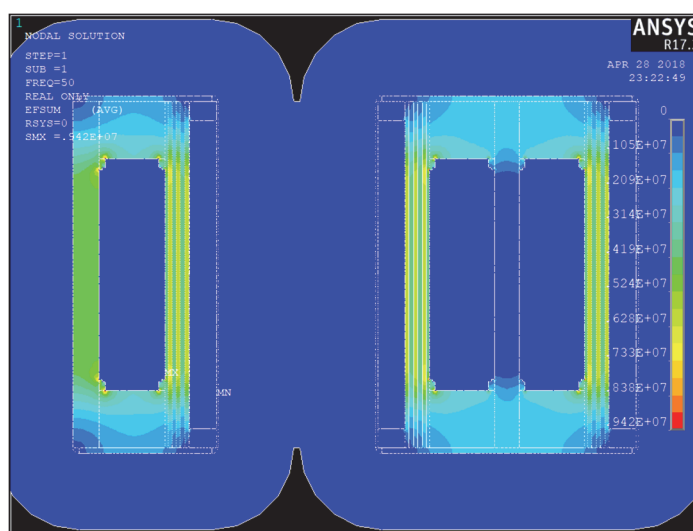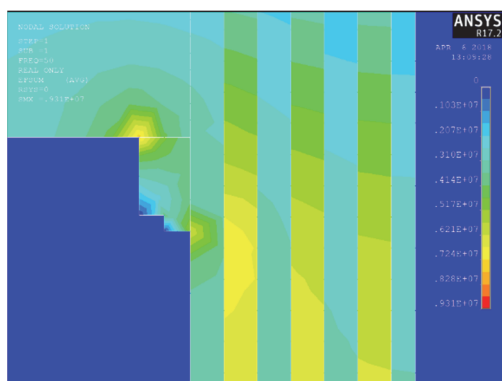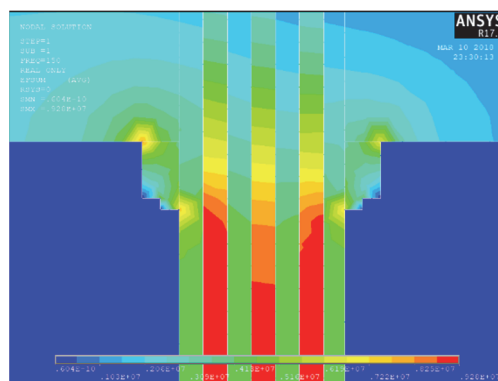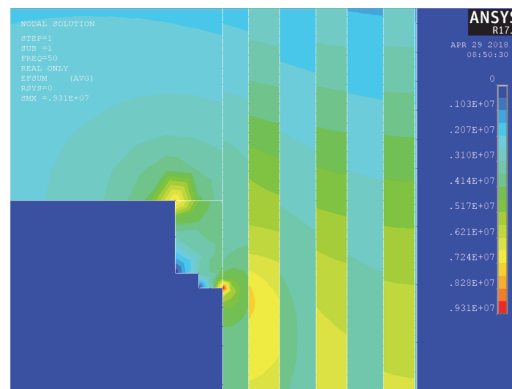

Figure 30. contour plot of electric field distribution in transformer insulation after reducing the insulation distances due to dielectric withstand test
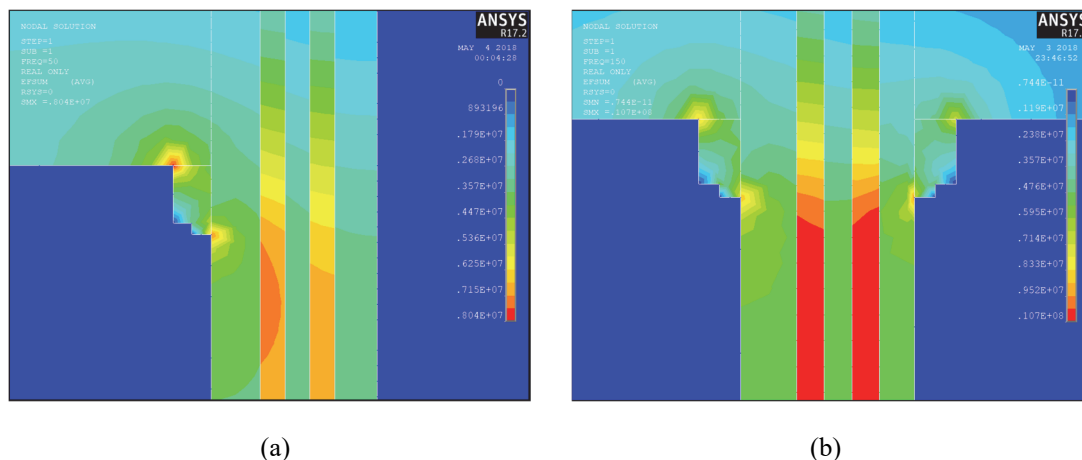

(a)   (b)

(c)

Figure 31. (a) electric field distribution at the H-C insulation. (b) electric field distribution at the H-H insulation. (c) electric field distribution at the H-L insulation

In the second proposed model, the insulation thicknesses kept unchanged, and oil gaps created among the pressboard layers in the H-C insulation and the H-H insulation by using oak wood ducts, these ducts will allow transformer oil circulation for cooling purpose, in addition the transformer oil is also a liquid insulator and this property used to enhance the transformer insulation. As a result of adding the oil gaps, the maximum value electric stress has been successfully reduced at the H-C insulation from 7.9kV/mm to 6.15kV/mm, also the maximum value of electric stress at the H-H insulation has been reduced from 7.28kV/mm to 6.59kV/mm. for the H-L insulation, the insulating diamond dotted paper is replaced by the aramid insulating paper, its relative permittivity when immersed in oil equals 4. And as a result the maximum value of electric stress at the H-L insulation reduced from 6.66kV/mm to 6.59kV/mm. figure 31 show the electric field distribution after adding the oil gaps and the new insulation material.

The third model included reducing the thickness of insulation of both the H-H insulation and the H-C insulation, and adding the oil gaps among the pressboard layers. The results obtained from the FE solution show reduction in the maximum values of electric stress at the end region of the high voltage windings at the H-H insulation had reduced to 6.22kV/mm, while the maximum value for the standard design of the transformer and the after reducing the thickness of insulation is 7.2kV/mm and 8.8kV/mm respectively. The electric stress value at the middle region of the H-H insulation has reduced to 3.75kV/mm as compared with the original value which equals to 4.5kV/mm. for the H-C insulation, the maximum value of electric stress has been reduced from 5.5kV/mm which the original value to 5.11kV/mm. and the electric stress in the middle region has been reduced to 2.4kV/mm. figure 32 shows the distribution of electric field at the end region of H-H insulation and the H-C insulation.

(a)   (b)

Figure 32. (a) electric field distribution at the end region of H-C insulation. (b) electric field distribution at the end region of H-H insulation

4. Conclusion

The conclusion that can become out from the presented work can be highlighted by the following points:

1. In fact most research paper and articles have discussed the calculation, the distribution, and analyzing the electric field in the core type distribution transformer, while this paper deals with calculation and analyzing the electric field distribution of the wound-core type distribution transformer.

2. The distribution of the electric field in insulation structure of the transformer under study has been successfully visualized and the maximum values of the electric field were calculated and located on the FE model.

3. The evaluation of the insulation system of the distribution transformer shows that the insulation system withstands properly and the dielectric strength of each insulating material used is much less than the break-down strength.

4. The observed FE model in this work can be used not only for evaluating the insulation thickness but also for other cases such as, changing the insulation thickness or using other types of insulating material. Thus, the observed model will help in saving time and cost in designing and testing the new prototype of the transformer.

5. After the reduction of the insulation thickness of the H-C insulation and the H-H insulation, the obtained results show that the insulation system works properly and no electric failure has taken place, and as a result this will reduce the transformer size, but this reduction may change the value of the transformer leakage impedance, but after redesigning the impedance value it was that its value has not been significantly changed.

References

Alireza, K., & Mehdi, V. (2008). *Power Transformers Internal Insulation Design Improvements Using Electric Field Analysis Through Finite-Element Methods.* https://doi.org/10.1109/TMAG.2007.912771

ANSYS 17.2 (2016). *Theory Reference for Mechanical APDL and Mechanical Applications.* Retrieved from http://www.ansys.com

Aydemir, A., & Özcan, K. (2005). *Electric Field Analysis of HVAC Testing Unit Using Finite Element Method.* Retrieved from https://www.researchgate.net/publication/237214793_electric_field_analysis_of_hvac_testing_unit_using_finite_element_method

Chakravorti, S. (2015). *Electric Field Analysis.* New York, NY.

Dyala Company for Electrical Industries, factory of distribution transformers. (1983). *Design Calculation Sheet of 250kVA distribution transformer.* Mitsubishi Electric Corporation

International Standard, IEC 60076-3 (2013). *Part 3: Insulation levels, dielectric tests and external clearances in air.*

Kosjenka, C., Žarko, J., & Željko, Š. (2013). *Analyzing Method Efficiency for Power Transformers Insulation Design.* https://doi.org/10.1109/EUROCON.2013.6625183

Mladen, M., Zeljko, S., & Branimir, C. (2013). *Power Transformer Main Insulation Design Improvement Using BEM and FEM.* https://doi.org/10.1109/EUROCON.2013.6625185

Naoki, H., Hiroshi, M., Hiroyuki, H., & Hitoshi, O. (2008). *Common Insulating Properties in Insulating Materials.* https://doi.org/10.1109/TDEI.2006.1624277

Pugazhendhi, S. C. (2013). Diagnosis on Mechanical and Electrical Properties of Cable Insulation PVC with Nanofiller. https://doi.org/10.1109/CATCON.2013.6737502

Youhua G., & Shaobo, W. (2012). *Research of Main Insulation Structure of Power Transformer Based on 3-D Electric Field.* https://doi.org/10.1109/APPEEC.2012.6307377

Youhua, G., Shaobo, W., & Dan, G. (2011). *Influence of Main Insulation Structure in Power Transformer to Electric Filed Distribution.* https://doi.org/10.1109/ICEMS.2011.6073835

Zeng, L. S., Xiao, P., Bai, S., Wu, Y., & Xia, Y. H. (2009). *Analysis of electric field of HV lead in Ultrahigh Voltage Power Transformer.* https://doi.org/10.1109/ICEMS.2009.5382906

Copyrights